THE JOURNAL OF BIOLOGICAL CHEMISTRY
Vol. 279, No. 10, Issue of March 5, pp. 9091–9096, 2004
© 2004 by The American Society for Biochemistry and Molecular Biology, Inc.
Printed in U.S.A.

ZmYS1 Functions as a Proton-coupled Symporter for Phytosiderophore- and Nicotianamine-chelated Metals*

Received for publication, October 28, 2003, and in revised form, December 23, 2003
Published, JBC Papers in Press, December 29, 2003, DOI 10.1074/jbc.M311799200

Gabriel Schaaf‡, Uwe Ludewig§, Bülent E. Erenoglu‡, Satoshi Mori¶, Takeshi Kitahara‖, and Nicolaus von Wirén‡**

From the ‡Institut für Pflanzenernährung, Universität Hohenheim, D-70593 Stuttgart, Germany, the §ZMBP-Pflanzenphysiologie, Universität Tübingen, Auf der Morgenstelle 1, D-72076 Tübingen, Germany, the ¶Laboratory of Plant Molecular Physiology, University of Tokyo, 1-1-1 Yayoi, Bunkyo-ku, Tokyo 113-8657, Japan, and the ‖Laboratory of Organic Chemistry, University of Tokyo, 1-1-1 Yayoi, Bunkyo-ku, Tokyo 113-8657, Japan

Among higher plants graminaceous species have the unique ability to efficiently acquire iron from alkaline soils with low iron solubility by secreting phytosiderophores, which are hexadentate metal chelators with high affinity for Fe(III). Iron(III)-phytosiderophores are subsequently taken up by roots via YS1 transporters, that belong to the OPT oligopeptide transporter family. Despite its physiological importance at alkaline pH, uptake of Fe-phytosiderophores into roots of wild-type maize plants was greater at acidic pH and sensitive to the proton uncoupler CCCP. To access the mechanism of Fe-phytosiderophore acquisition, *ZmYS1* was expressed in an iron uptake-defective yeast mutant and in *Xenopus* oocytes, where ZmYS1-dependent Fe-phytosiderophore transport was stimulated at acidic pH and sensitive to CCCP. Electrophysiological analysis in oocytes demonstrated that Fe-phytosiderophore transport depends on proton cotransport and on the membrane potential, which allows ZmYS1-mediated transport even at alkaline pH. We further investigated substrate specificity and observed that ZmYS1 complemented the growth defect of the zinc uptake-defective yeast mutant *zap1* and transported various phytosiderophore-bound metals into oocytes, including zinc, copper, nickel, and, at a lower rate, also manganese and cadmium. Unexpectedly, ZmYS1 also transported Ni(II), Fe(II), and Fe(III) complexes with nicotianamine, a structural analog of phytosiderophores, which has been shown to act as an intracellular metal chelator in all higher plants. Our results show that ZmYS1 encodes a proton-coupled broad-range metal-phytosiderophore transporter that additionally transports Fe- and Ni-nicotianamine. These biochemical properties indicate a novel role of YS1 transporters for heavy metal homeostasis in plants.

Although iron is the second most abundant metal in the earth's crust, the bioavailability of this essential micronutrient is extremely low. Many microorganisms and graminaceous plant species overcome this problem by secreting siderophores, which are hydroxamate-, hydroxypyridonate-, catechol-, or aminocarboxylate-type chelators with a particular high affinity for Fe(III) (1, 2). After mobilization of Fe(III), *e.g.* from sparingly soluble precipitates, siderophore-bound iron is subsequently taken up by specific transport systems, which have been well characterized in prokaryotic organisms (3). Yeast or dicotyledonous and non-graminaceous monocotyledonous plants increase proton secretion by H^+-ATPases as well as Fe(III) reduction capacity by ferric chelate reductases at the root plasma membrane and induce the Fe(II) transporter IRT1 (4). This reduction-based strategy, however, is prone to inhibition by high pH and elevated bicarbonate levels in calcareous soils, due to the pH dependence of chemical Fe(III) solubilization and enzymatic Fe(III) reduction (5). By contrast, graminaceous plant species constitutively express the reduction-dependent pathway for iron uptake at a comparatively low level, but enhance capacities for phytosiderophore release and Fe(III)-phytosiderophore uptake under iron deficiency (6). Physiological studies showed that Fe-phytosiderophore transport in graminaceous plants is unaffected by the presence of strong Fe(II) chelators, such as BPDS (6), but recognizes the backbone structure of mugineic acid-derived phytosiderophores, which are aminocarboxylate-type, hexadentate Fe(III) chelators (Refs. 1 and 7 and Fig. 1). In roots of maize high-affinity Fe(III)-phytosiderophore uptake is required to produce non-chlorotic, healthy plants, and is strongly dependent on the *YS1* gene product (8). Transposon-tagging of the *YS1* gene in maize allowed to identify ZmYS1 as a highly hydrophobic protein with 14 putative transmembrane-spanning domains that confers growth of the iron uptake-defective yeast mutant *fet3 fet4* on phytosiderophore-bound iron, even in the presence of the Fe(II) chelator BPDS[1] (9). This study confirmed earlier uptake experiments with double-labeled Fe-phytosiderophores in the *ys1* mutant indicating a stochiometric uptake of metal and ligand (10). The non-reductive transport pathway of Fe-phytosiderophores seems especially effective at alkaline pH and very low concentrations of Fe(III)-phytosiderophore complexes (11, 12).

Although showing high affinity for ferric, phytosiderophores of the mugineic acid family do also chelate other heavy metals. Phytosiderophore-enriched root exudates efficiently mobilized copper, manganese, and zinc as well as other non-essential heavy metals (13, 14). Moreover, uptake studies with labeled metal-phytosiderophores indicated that

* This research was supported by Deutsche Forschungsgemeinschaft (DFG) with a grant to N. von Wirén (WI1728-1). The costs of publication of this article were defrayed in part by the payment of page charges. This article must therefore be hereby marked "*advertisement*" in accordance with 18 U.S.C. Section 1734 solely to indicate this fact.

** To whom correspondence should be addressed: Institut für Pflanzenernährung, Universität Hohenheim, D-70593 Stuttgart, Germany. Tel.: 49-711-459-2344; Fax: 49-711-459-3295; E-mail: vonwiren@uni-hohenheim.de.

[1] The abbreviations used are: BPDS, bathophenanthroline disulfonate; DMA, 2′-deoxymugineic acid; NA, nicotianamine; MES, 4-morpholineethanesulfonic acid.

Downloaded from http://www.jbc.org/ by guest on June 8, 2020

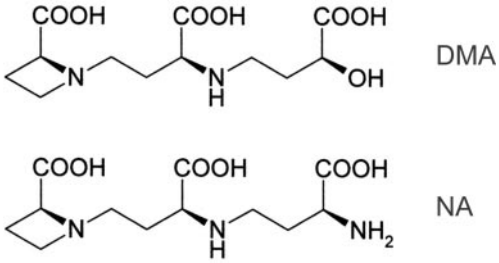


FIG. 1. **Structures of DMA and NA.**

barley roots possess uptake activities for phytosiderophore-complexed zinc and copper (7, 15) and that ZmYS1 is responsible for the import of Zn(II)-phytosiderophores in maize roots (16). Thus, the plant phytosiderophore system could potentially also serve for the acquisition of metals other than iron, which is supported by the observation that phytosiderophore release is not only triggered under iron-deficient growth conditions, but also induced under zinc deficiency (15, 17). In plants, metal-phytosiderophore uptake is not only important for covering the micronutrient demand of the plant, but might also be important for employing plants in future for phytoremediation purposes.

In the dicotyledonous plant *Arabidopsis thaliana* eight ZmYS1 homologs (*AtYSL1–8*) have been identified (9). Since the release of phytosiderophores has so far not yet been observed in dicotyledonous plants, it is possible that YSL proteins function to transport metal-nicotianamine (NA) chelates. Nicotianamine, which occurs in all higher plants, is structurally similar to phytosiderophores and serves as a precursor in their biosynthetic pathway (Ref. 18 and Fig. 1). A strong link between NA and iron metabolism is reflected in the NA-less tomato mutant *chloronerva* that shows severe symptoms of iron deficiency due to a deletion in a gene encoding nicotianamine synthase (19). Furthermore, NA has been shown to chelate not only Fe(III) but also Fe(II), in particular at higher pH, which may allow it to serve as an intracellular Fe(II) scavenger thereby protecting the cell from Fe(II)-mediated oxidative damage (20). The recent success of chemical synthesis of NA (21) allowed us also to investigate metal-NA chelate transport.

In order to understand iron-phytosiderophore transport under alkaline conditions and to characterize metal and ligand specificity by the ZmYS1 transporter in maize, we expressed ZmYS1 in two heterologous systems and verified its transport properties in the *ys1* maize mutant. We found that ZmYS1 mediates transport of phytosiderophore-bound Fe(III) and other metals by H^+-coupled cotransport and permeates also NA-complexed Fe(II), Fe(III), and Ni(II).

EXPERIMENTAL PROCEDURES

Plasmids, Yeast Strains, and Growth Conditions—Plasmid preparation, restriction enzyme digestion, and DNA ligation were performed using standard methods (22). The *ZmYS1* open reading frame containing a 32-bp 5′-untranslated region was subcloned from pYPGE15 (9) into the yeast expression vector pDR196 (23) and the oocyte expression vector pOO2 (24) using EcoRI/XhoI restriction sites. The *fet3 fet4* mutant DEY1453 (MATa/MATα ade2/+can1/can1 his3/his3 leu2/trp1/trp1 ura3/ura3 fet3-2:HIS3/fet3-2:HIS3/fet4-1:LEU2/fet4-1:LEU2) (25), the *zap1* mutant (BY4741; Mat a; his3Δ1; leu2Δ0; met15Δ0; ura3Δ0; YJL056c::kanMX4; acc no Y01367 from Euroscarf) (www.uni-frankfurt.de/fb15/mikro/euroscarf/index.html) and its isogenic wt (BY4741; Mat a; his3Δ1; leu2Δ0; met15Δ0; ura3Δ0; acc no Y00000 from Euroscarf) were used for yeast complementation. Media were prepared using standard recipes (22, 26).

To support growth of the *fet3 fet4* mutant, solid YNB medium contained additionally 30 μM $FeCl_3$, while the liquid YPD medium was acidified to pH 5.0 with HCl. Yeast was transformed with either pDR196 or pDR196-*ZmYS1* using the LiAc method (27), and transformants were selected on uracil-deficient YNB medium containing 0.1% arginine as nitrogen source and the appropriate supplements.

For growth tests a single colony from BY4741 and *fet3 fet4* transformants was washed in 1 ml of 10× TE (pH 7.5) and resuspended in sterile MQ water to obtain an OD of 0.09. Cells were streaked on uracil-deficient YNB medium, containing 0.1% arginine, 3% glucose, 0.01% tryptophane, histidine, methionine, leucine, and the respective iron source. For complementation of the *zap1* mutant, cells were streaked on a modified LIM medium (28) without sodium citrate, zinc sulfate, and ammonium, but supplemented with 0.1% arginine, 3% glucose, 0.01% histidine, methionine, and leucine, 50 mM MES/Tris (pH 7.0) and the respective zinc source.

For uptake experiments single colonies of transformed BY4741 cells were cultured in liquid YNB medium containing 3% glucose, the appropriate supplements and 30 μM $NiSO_4$, harvested at mid-log phase, washed at 4 °C in ice cold uptake buffer consisting of 3% glucose, 40 mM NaH_2PO_3 (pH 6.5) and resuspended on ice in uptake buffer to obtain OD 12. Before the uptake experiment, cells were incubated for 15 min at 30 °C (500 rpm). Uptake was started by addition of 1 volume of solution containing 3% glucose, 100 mM MES/Tris (pH 6.5) and the respective ^{63}Ni(II)-chelate (specific activity 143 Ci mol^{-1}). 100 μl of uptake reaction was diluted in 10 ml of 10 mM EDTA (pH 6.5) and filtered (Whatman, 1822 025) before analyzing filter membranes by scintillation counting.

Electrophysiological Studies in Xenopus laevis Oocytes—Capped cRNA was transcribed from pOO2-ZmYS1 *in vitro* using the mMessage mMachine kit (Ambion, Austin, TX), after linearization of the plasmid with Eco72I. Oocyte experiments were performed as described in (29). Metal-chelate-induced currents in oocytes were detected by two electrode voltage clamp 3 days after cRNA injection.

Preparation of Metal Chelates—Deoxymugineic acid (DMA) was produced, and NA was chemically synthesized as described previously (16, 21). Fe-DMA was prepared by mixing appropriate amounts of a 10 mM $FeCl_3$ solution, pH <2, and MES/Tris buffer and, if not indicated otherwise, with a 10-fold excess of DMA for 2–3 h at RT. Fe(II)-NA was obtained by mixing a freshly prepared Fe(II) stock solution consisting of 10 mM $FeCl_2$ and 20 mM ascorbate in 200 mM MES/Tris, pH 7.0 or 7.5, with the appropriate amount of a 10 mM NA solution and MES/Tris buffer, pH 7.0 or 7.5, followed by 10 min of incubation at 65 °C. According to this procedure successful complex formation had been verified (20, 35). Formation of the Fe(II)-NA complex was monitored by disappearance of the purple Fe-ascorbate complex. The Fe(III)- and Ni(II)-NA complexes were prepared similarly by dissolving $FeCl_3$ or $NiSO_4$ in 10 mM HCl to obtain a 10 mM metal solution, and mixing with the appropriate amount of MES/Tris buffer and NA, followed by incubation at 65 °C for 10 min. In all solutions NA was in 20% excess if not indicated otherwise. All chelate solutions were centrifuged or filtered (0.2 μm, Schleicher & Schuell) to remove precipitated iron hydroxides. Iron concentrations of supernatants or filtrates were verified by AAS or scintillation counting.

^{59}Fe-labeled Fe-phytosiderophore Uptake Studies in Maize—Maize plants were precultured and subjected to uptake studies using ^{59}Fe-labeled Fe-DMA (8, 16). CCCP was added from 1 mM or 10 mM stock solutions in methanol to uptake solutions to final concentrations of 10 or 100 μM (solutions w/o CCCP contained methanol alone). Uptake solutions were buffered with MES/Tris or HEPES.

RESULTS

Fe-Phytosiderophore Transport in Maize Roots Is pH-dependent—Since graminaceous plant species are dependent on Fe(III)-phytosiderophore uptake in particular at alkaline soil pH, uptake of ^{59}Fe-labeled Fe(III)-DMA was compared in wild type (Alice) and *ys1* mutant plants at different pH values of the uptake solution. At alkaline pH (pH 7.5) uptake rates of Fe(III)-DMA were 5-fold higher in wild type maize compared with *ys1* mutant plants. However in wild type maize decreasing pH caused an increase in uptake which was almost 2-fold higher at pH 4.5 compared with pH 7.5 (Fig. 2*A*). The majority of this Fe(III)-DMA uptake could be ascribed to ZmYS1, since uptake rates in the *ys1* mutant were five to ten times lower and did not change with external pH. To confirm a pH dependence of Fe-phytosiderophore uptake further, the effect of the proton uncoupler CCCP on root uptake of labeled Fe(III)-DMA was tested in Fe-deficient wild-type plants. Addition of CCCP at concentrations of 10 and 100 μM led to a 10–20-fold decrease in

Downloaded from http://www.jbc.org/ by guest on June 8, 2020

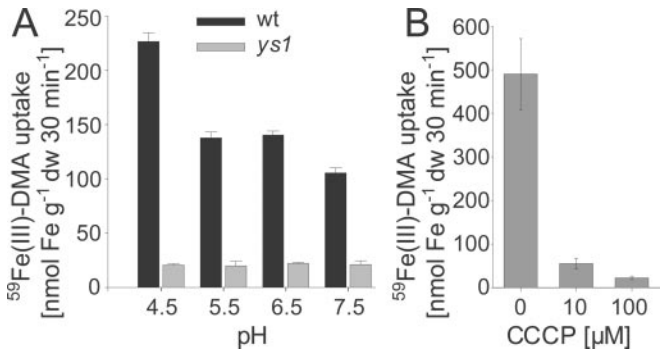


FIG. 2. **Fe(III)-DMA uptake in roots of maize is pH-dependent and sensitive to CCCP.** *A*, influence of pH on Fe(III)-DMA uptake. Fe-DMA concentration was 1 μM (DMA in 1.2-fold molar excess), pH was adjusted to 4.5, 5.5, 6.5, or 7.5 using MES/Tris. 15-day-old Fe-deficient maize plants (cv. Alice and *ys1*) were supplied with ^{59}Fe-labeled Fe(III)-DMA for 30 min. *B*, effect of CCCP on Fe-DMA uptake in roots of Alice. 10 or 100 μM CCCP (dissolved in methanol) were added to nutrient solutions containing 5 μM ^{59}Fe-labeled Fe-DMA; control plants received methanol w/o CCCP. *Bars* indicate mean values ± S.D., $n = 4$.

Fe(III)-DMA uptake (Fig. 2*B*), suggesting a dependence of Fe(III)-DMA transport on the proton gradient across the root plasma membrane.

Transport Properties of ZmYS1 in Yeast—ZmYS1 has been shown to complement growth of the *fet3 fet4* mutant (9), which is defective in high and low affinity iron transport and cannot grow on Fe-limited medium (30). As expected, *fet3 fet4* cells transformed with pDR196-ZmYS1 grew well on medium containing 7.5 μM Fe(III)-2′-DMA, whereas transformants with the empty vector did not (Fig. 3*A*). Growth complementation was pH-dependent. ZmYS1 transformants appeared earlier (data not shown), and colony number increased with decreasing pH (Fig. 3*A*).

To test ligand specificity of ZmYS1-mediated transport, ZmYS1-transformed *fet3 fet4* cells were grown on NA-chelated iron. After 7-days growth complementation was achieved by 40 μM of either Fe(II)-NA or Fe(III)-NA (Fig. 3*B*), while growth was not complemented using 7.5 μM Fe-NA (data not shown). With supply of 30 μM $FeCl_3$ differences between yeast transformants disappeared (Fig. 3*C*).

Zn(II)-phytosiderophore transport was investigated employing the zinc uptake-defective yeast strain *zap1*, which carries a deletion in the zinc-responsive transcriptional activator *Zap1* (31) and does not grow on modified LIM medium containing less than 400 μM zinc when transformed with pDR196 alone (Fig. 3*D*). Transformation of *zap1* with pDR196-*ZmYS1*, however, permitted growth on 0.7 mM Zn(II)-DMA as zinc source, showing that ZmYS1 also transports phytosiderophore-chelated zinc (Fig. 3*D*).

To investigate ZmYS1-mediated transport of nickel complexes, we first examined time-dependent uptake of ^{63}Ni-DMA in the wt yeast strain BY4741. Little uptake was detected at 4 °C for either ZmYS1-expressing or control cells (Fig. 4*A*). At 30 °C, ZmYS1 expression led to an almost linear increase in ^{63}Ni accumulation over 20 min, while control cells hardly accumulated any ^{63}Ni. Nickel(II)-DMA uptake activity stopped immediately after addition of CCCP, while cells receiving the solvent alone continued to accumulate ^{63}Ni(II)-DMA (Fig. 4*B*). Uptake activity of ^{63}Ni(II)-NA was also CCCP-sensitive and increased almost linearly over time, though at a 3-fold lower rate (Fig. 4*C*). Concentration-dependent uptake of both nickel complexes in a range between 1 and 300 μM yielded saturable kinetics, and Lineweaver-Burk transformation allowed calculatation of a K_m of ZmYS1 for Ni(II)-NA of 165 μM compared with a K_m of 19 μM for Ni(II)-DMA (Fig. 4*D*). Hence nickel was transported by ZmYS1 in a similar manner to iron, *i.e.* as a DMA- or NA-chelate and in a CCCP-sensitive manner.

Electrophysiological Characterization of ZmYS1-mediated Transport in Oocytes—To study the transport mechanism employed by ZmYS1 in more detail, the protein was expressed heterologously in *Xenopus laevis* oocytes. Oocytes were voltage-clamped to −70 mV in choline-based buffer solution at pH 6.0 and then superfused with buffer containing different concentrations of Fe(III)-DMA. In oocytes injected with cRNA encoding ZmYS1, currents induced by Fe(III)-DMA corresponded to the net influx of positive charge, reversed after withdrawal of substrate and were voltage and concentration-dependent (Fig. 5*A*). Currents were absent in water- or non-injected control oocytes (data not shown). Fe(III)-DMA-dependent currents increased with more negative voltage and increasing substrate concentrations up to ~25 μM Fe(III)-DMA (Fig. 5*B*). Thus, Fe(III)-DMA transport was saturable, and the Fe(III)-DMA concentration that permitted half-maximal uptake was between 5 and 10 μM with the tendency to decrease at more positive voltage (Fig. 5*C*). A decreasing K_m with less negative voltage indicates binding of a negatively charged substrate to the transport protein.

Fe(III)-DMA-induced currents strongly depended on external pH. Highest currents were obtained at pH 5.0 and gradually decreased by increasing the pH to 9.5 (Fig. 6*A*). Plotting substrate-induced currents against H^+ concentrations showed that Fe(III)-DMA-induced currents increased up to proton concentrations of 100 nM, corresponding to a pH of 7, but saturated at higher proton concentrations (Fig. 6*B*). Replacing choline by sodium (100 mM, pH 9.5) did not stimulate transport, indicating that sodium could not substitute protons to drive metal-chelate uptake (Fig. 6*A*).

Since yeast uptake experiments provided evidence that ZmYS1 might also transport other heavy metals chelated with phytosiderophores (Fig. 4), different metal-chelates were tested for the induction of currents in *ZmYS1*-injected oocytes. When supplied at 100 μM external concentration, Ni(II)-, Zn(II)-, and Cu(II)-DMA provoked currents of similar size to those achieved with Fe(III)-DMA (Fig. 7*A*). By contrast, Mn(II)- and Cd(II)-bound DMA induced significantly smaller currents and negligible currents were induced by the unchelated ligand. Ferrous and ferric complexes with the synthetic chelator EDTA or unchelated metals (data not shown) induced little if any current. Since ZmYS1 might be saturated at <100 μM, currents were also assayed at 5 μM corresponding to the K_m for Fe(III)-DMA (Fig. 5*C*). Currents induced by Ni(II)-, Zn(II)-, and Cu(II)-DMA were smaller relative to those induced by Fe(III)-DMA, while currents induced by Mn(II)- and Cd(II)-DMA approached zero (Fig. 7*B*), indicating that Cd- and Mn-phytosiderophore transport by ZmYS1 will be relatively insignificant in the presence of more competitive metals like iron, nickel, zinc, and copper. Smaller currents induced by 5 μM Ni(II)-DMA compared with 5 μM Fe(III)-DMA were consistent with the higher K_m value of ZmYS1 for Ni(II)-DMA (Fig. 4*D*) compared with Fe(III)-DMA (Fig. 7*A*). Currents induced by DMA-chelated Fe(III) were then compared with NA-chelated iron at a concentration of 5 μM, clearly showing that ZmYS1 transports Fe(III)-DMA more efficiently than Fe(II)- or Fe(III)-NA (Fig. 7*B*). Together with the observation in yeast, where ZmYS1-mediated uptake of Ni(II)-DMA was higher than uptake of Ni(II)-NA, we concluded that metal-DMA complexes are more favored substrates for ZmYS1 compared with metal-NA complexes. At higher concentration and more negative membrane potential a discrimination between Fe(II)- and Fe(III)-NA transport could be achieved. Currents induced by 100 μM Fe(II)-NA increased steeply with voltage and were 3-fold larger than those for Fe(III)-NA (Fig.

Downloaded from http://www.jbc.org/ by guest on June 8, 2020

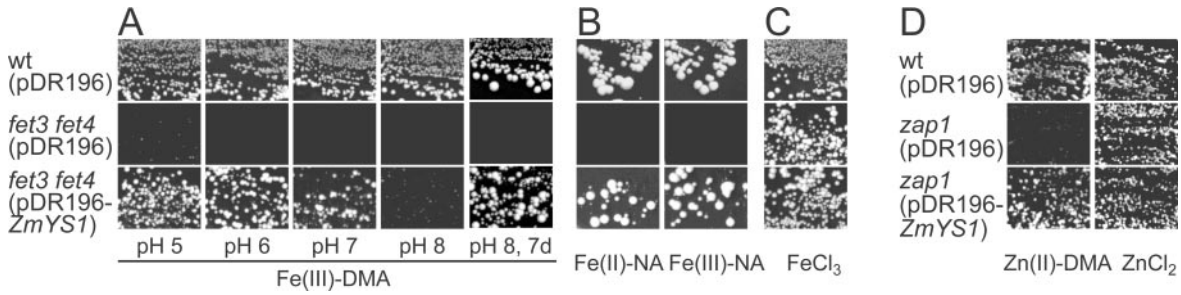


FIG. 3. **Functional complementation of the growth defect of the yeast *fet3 fet4* mutant by ZmYS1.** Wt yeast (Y00000, Euroscarf) was transformed with pDR196, the *fet3 fet4* (DEY1453) mutant was transformed with either pDR196 or pDR196-*ZmYS1*. Transformants were plated on YNB medium supplemented with 7.5 μM Fe-DMA, 50 mM MES/Tris at pH 5, 6, 7 or 8 (*A*); or with 40 μM Fe(II)-NA (left) or 40 μM Fe(III)-NA (right) both in 50 mM MES/Tris at pH 7 (*B*); or with 30 μM $FeCl_3$ at pH 5.5 (*C*). Plates were incubated at 30 °C for 4 (*A* and *C*) or 7 (in *A* for pH 8, and *B*) days. *D*, functional complementation of the growth defect of the yeast *zap1* mutant. Wt yeast (Y00000, Euroscarf) and the *zap1* mutant (Y01367, Euroscarf) were transformed with pDR196 or pDR196-*ZmYS1* and plated on modified LIM medium supplemented with 700 μM Zn(II)-DMA (DMA in 2-fold molar excess) or 1 mM $ZnCl_2$. Plates were incubated at 30 °C for 6 days.

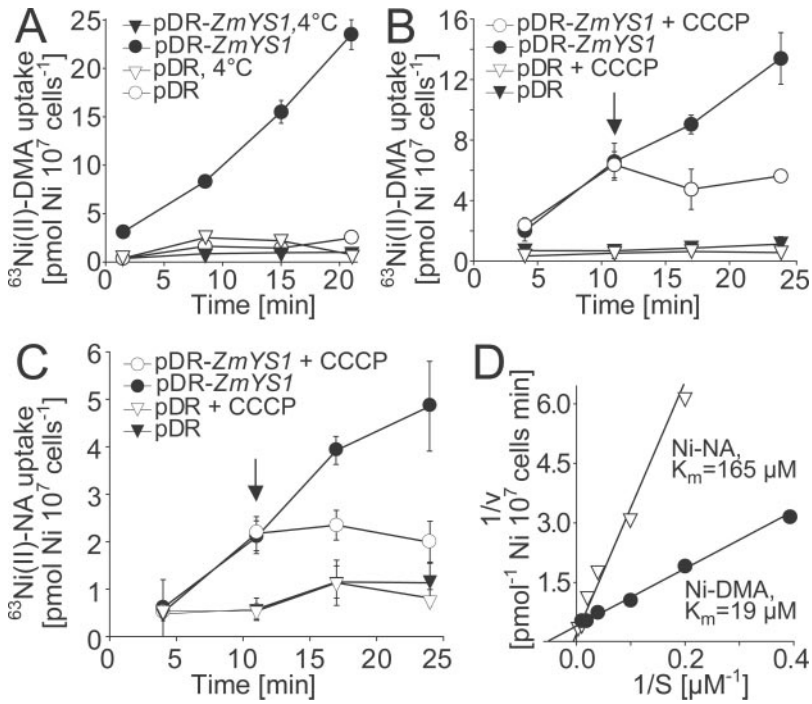


FIG. 4. **ZmYS1 mediates transport of Ni(II)-DMA and Ni(II)-NA in yeast.** OD12 cells of BY4741 were preincubated 15 min at 30 °C (or 4 °C) before uptake was started by addition of 1 vol. ^{63}Ni-chelate solution (pH 6.5). *A*, ZmYS1 mediates transport of Ni(II)-DMA in a temperature-sensitive manner. Yeasts harboring pDR196 or pDR196-*ZmYS1* were incubated at 30 °C or 4 °C in uptake solution containing 6 μM ^{63}Ni-labeled Ni(II)-DMA. *B* and *C*, ZmYS1-mediated transport of Ni(II)-DMA and Ni(II)-NA is sensitive to CCCP. Time-dependent uptake of nickel from 3.5 μM ^{63}Ni-labeled Ni(II)-DMA (*B*) or Ni(II)-NA (*C*). CCCP was added after 11 min (*arrow*) to a final concentration of 100 μM, while control treatments received Me_2SO alone. Symbols represent mean values ± S.D., $n = 3$. *D*, Lineweaver-Burk transformation of concentration-dependent uptake rates of Ni(II)-DMA and Ni(II)-NA.

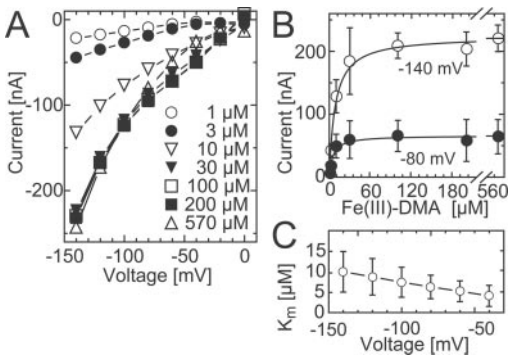


FIG. 5. **Voltage and concentration dependence of Fe(III)-DMA-induced currents in ZmYS1-expressing oocytes.** *A*, Fe(III)-DMA induced currents increased with more negative voltage and external substrate concentration. *B*, Fe(III)-DMA-induced currents at −140 or −80 mV saturated above 25 μM, $n = 3$. *C*, K_m values for ZmYS1-mediated Fe(III)-DMA transport at pH 6.0 were determined at different membrane potentials.

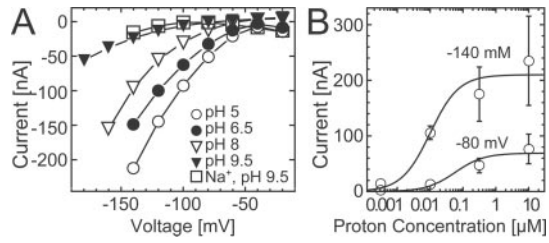


FIG. 6. **Proton dependence of Fe(III)-DMA-induced, ZmYS1-mediated currents.** *A*, oocytes were held at −70 mV and superfused with 50 μM Fe(III)-DMA at increasing pH of the bathing solution. At pH 9.5 choline chloride was substituted by 100 mM NaCl. *B*, proton saturation of Fe(III)-DMA-induced currents. Oocytes were held at −80 mV or −140 mV and Fe(III)-DMA-induced currents at 50 μM were plotted against proton concentration.

7*C*). The induction of currents by NA complexes with both iron forms clearly agreed with the growth complementation of ZmYS1-transformed yeast cells on Fe(II)- and Fe(III)-NA (Fig. 3*B*).

DISCUSSION

ZmYS1 Mediates H^+-coupled High Affinity Fe-Phytosiderophore Transport—In three different systems we observed that ZmYS1-mediated Fe(III)-DMA transport depends on the availability of protons: (i) in maize roots Fe(III)-DMA uptake was severely inhibited by CCCP, and the contribution of ZmYS1 to transport of the iron chelate increased with the concentration of external protons (Fig. 2); (ii) in yeast, low pH values

Downloaded from http://www.jbc.org/ by guest on June 8, 2020

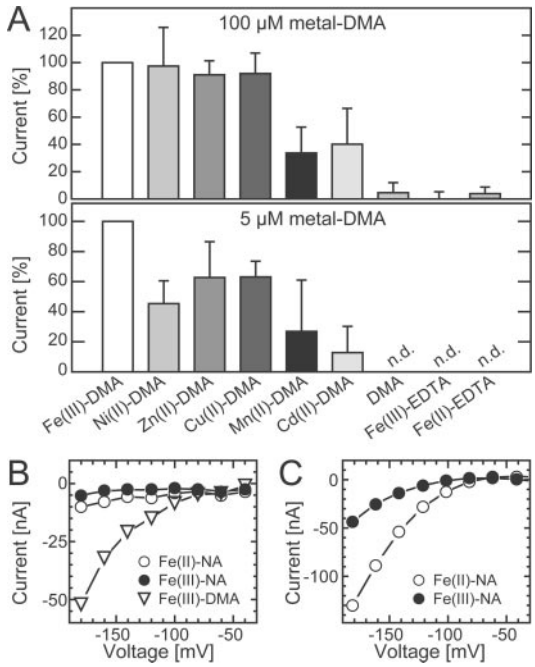


FIG. 7. **Broad specificity of metal-chelate transport by ZmYS1.** *A*, normalized currents ± S.D. at pH 6.0 from 3–4 individual oocytes were analyzed at −120 mV and 100 µM metal-DMA (*top*) or at −140 mV and 5 µM metal-DMA (*bottom*). Fe(III)-DMA-induced currents were set as 100%. *B*, voltage dependence of Fe(III)-DMA *versus* Fe(III)- and Fe(II)-NA-induced currents at 5 µM chelate, pH 6.0. *C*, Fe(II)- and Fe(III)-NA-induced currents are distinct at 100 µM chelate concentration, pH 7.5, and more negative voltage.

improved growth complementation by ZmYS1 of the iron uptake-defective yeast mutant *fet3 fet4* (Fig. 3*A*) and uptake of ^{63}Ni(II)-DMA was strongly inhibited by CCCP (Fig. 4*B*); and (iii) oocytes expressing ZmYS1 exhibited a positive inwardly rectifying and voltage-dependent current in response to supply with negatively charged Fe(III)-DMA and this current was proton dependent (Figs. 5 and 6). Considering the almost stochiometric uptake of double-labeled ^{59}Fe- and ^{65}Zn-^{14}C-DMA by maize roots (8, 16), we conclude that ZmYS1 represents a H^+-Fe(III)-phytosiderophore cotransporter. These data provide the first description of the transport mechanism employed by a member of the OPT family of oligopeptide transporters. In view of the pH and CCCP sensitivity of oligopeptide transport in yeast by ScOPT1 (32, 33), which belongs to a different cluster within the OPT family (34), it is likely that energization by H^+-cotransport also holds true for other OPT members.

Proton cotransport is surprising in view of the environmental conditions, under which the uptake of Fe(III)-phytosiderophores has to take place. The release of phytosiderophores by graminaceous species is enhanced as a response to low availability of soluble iron, which naturally occurs at high pH, such as is found in calcareous soils. In contrast to plants employing reduction-dependent iron acquisition, iron deficiency in grasses shows little if any correlation with elevated bicarbonate concentrations (12), since iron acquisition does not rely on an Fe(III) reduction step. Our investigations uncovered another factor that contributes to more efficient iron acquisition in grasses: coupling the transport of Fe-phytosiderophores, which are negatively charged at neutral pH (35), to protons allows efficient root uptake even at high soil pH, because transport of the proton-coupled substrate can be driven as long as the overall difference of the electrochemical potential remains negative. This is emphasized by the Fe-DMA-induced currents in ZmYS1-expressing oocytes at pH 9.5, where currents appeared already at membrane potentials below −120 mV (Fig. 6*A*). Since the membrane potentials of root cells in grasses are usually between −120 and −180 mV, Fe-phytosiderophore uptake can still be driven until the availability of protons as a co-substrate becomes limiting. In oocytes proton availability limited Fe-DMA transport between pH 7 and 9.5 (Fig. 6*B*); but in soil-grown plants proton limitation probably occurs even at higher soil pH, because P-type ATPase-mediated proton extrusion may generate a local pH gradient favoring substrate-proton cotransport (36). Thus, even at high proton buffering capacities in bicarbonate-rich soils, the electrochemical potential drives accumulation mainly by generating a strongly negative membrane potential. Under these conditions ZmYS1 can exhibit a high substrate affinity (K_m of 5–10 µM, Fig. 5*C*) that would address the micromolar phytosiderophore concentrations found in the rhizosphere of grasses (11).

Several plant transporters employ proton cotransport for negatively charged substrates, such as sulfate, nitrate or amino acids (37, 38). Fe(III)-DMA complexes are negatively charged at neutral pH, while at pH 5 the majority of complexes is uncharged (35). The slight tendency of ZmYS1 to increase the affinity for DMA-complexed Fe(III) at more positive voltage (Fig. 5*C*) tempts us to speculate that the negatively charged substrate and protons bind to different sites of ZmYS1 prior to transport. Since Fe(III)-DMA transport generated a positive inward current, at least two protons are cotransported with each complex. Interestingly, the net current with different saturating metal-complex concentrations was similar irrespectively of the valency of substrate charge (Fig. 7*A*). As phytosiderophore complexes with divalent cations such as copper, zinc, or nickel, are predicted to carry two negative charges at neutral pH (35), the positive inward current demands that at least three protons are cotransported with these substrates.

ZmYS1 Shows a Broad Metal Specificity—Growth complementation and oocyte transport studies clearly showed that ZmYS1 also transports phytosiderophore-chelated Zn(II). This has been substantiated *in planta* by lower uptake rates of ^{65}Zn-phytosiderophores in the *ys1* mutant compared with wild type maize (16). Since phytosiderophore release is also enhanced under zinc deficiency in several graminaceous species, zinc-phytosiderophore transport by ZmYS1 most likely represents one part of a concerted adaptive response to low zinc availability. Thus, phytosiderophore release, metal chelation and chelate uptake apply for iron and zinc, which is ecologically reasonable, since poor availability of both metal micronutrients can limit plant growth on calcareous soils (12). However, ZmYS1 also transported phytosiderophore-chelated nickel and copper at a similar rate to iron and zinc (Fig. 7*A*), although low availabilities of nickel and copper are apparently not limiting growth factors in calcareous soils. The specificity of phytosiderophore-mediated metal chelation and transport might thus be regarded as low, suggesting that metal-chelate transport by ZmYS1 primarily depends on the probability of complex formation and on regulation of ZmYS1. Since metal-phytosiderophore transport by ZmYS1 shows a similar poor selectivity for iron, as does metal transport by the major iron transporter IRT1 (30, 39), for which a complex regulation at the transcript level by iron and cadmium and at the protein level by iron and zinc was found (40), it might be expected that *ZmYS1* also responds to the availability of multiple metal elements. The broad range of metal transport therefore suggests that regulation of *ZmYS1* by other metals is required as a prerequisite for plants to maintain metal ion homeostasis. On the other hand, the broad metal specificity of ZmYS1 opens up the possibility that the demand of other micronutrients, such as nickel, might also be satisfied by the phytosiderophore system and paves the way to employ phytosiderophore-releasing species for phytore-

Downloaded from http://www.jbc.org/ by guest on June 8, 2020

mediation. Since phytosiderophore-overproducing rice plants have already been generated and shown to increase iron acquisition on calcareous soils (41), we suggest to test such engineered plant lines also for the hyperaccumulation of other heavy metals.

ZmYS1 Also Transports Fe- and Ni-nicotianamine—In contrast to phytosiderophores NA is not only synthesized by graminaceous plant species but by all higher plants and appears essential for chlorosis-free plant growth (19, 42). Due to the structural similarity of NA with phytosiderophores, we reasoned that ZmYS1 or ZmYS1-related proteins might also transport Fe-NA. Indeed, in both heterologous systems ZmYS1 transported also NA-chelated iron and Ni(II) (Figs. 3*B*, 4, and 7). Fe- and Ni-NA transport by ZmYS1 is of particular physiological importance, since NA is believed to fulfill a physiological role, which is different from phytosiderophores. Based on the formation of stable complexes between NA and Fe(II) or Fe(III) (20), the occurrence of NA in aqueous extracts of leaves and roots (43) and the likely accumulation of Fe-NA complexes in the cytoplasm and the vacuole (44), NA may find its physiological role in iron chelation for the intracellular delivery of iron and long-distance trafficking of iron, zinc, and copper (44). NA-chelated Fe(II), which exhibits a relatively high kinetic stability (20), could even provide the opportunity for membrane transport of a ferrous iron chelate by maintaining a low risk for the generation of free superoxide radicals compared with the transport of free ferrous iron as mediated by IRT- or NRAMP-family transporters (39, 45). Since *Arabidopsis* possesses eight ZmYS1-like genes (*AtYSL1–8*) (9) but does not synthesize phytosiderophores, transport of Fe-NA might represent a major function for this transporter family in dicotyledonous plant species. Thus, YS1 and YSL proteins might act in a complementary manner to IRT and NRAMP transporters, since membrane transport could be mediated without involving a reduction step.

An alternative physiological role of YS1 and YSL proteins is indicated by our finding that ZmYS1 mediates transport of Ni(II)-NA (Fig. 4). Supported by the observation that one NA synthase gene from maize, *ZmNAS3*, is up-regulated by iron sufficiency, which provides evidence for NA synthesis independent of phytosiderophore biosynthesis (46), a novel role for NA in heavy metal transport and detoxification is indicated. Indeed, recent investigations on the physiological basis of nickel tolerance in the hyperaccumulator species *Thlaspi caerulescens* identified enhanced chelation of Ni(II) by NA in the xylem as a response to toxic levels of external nickel (47). This response implies the existence of membrane transporters for NA-chelated Ni(II), that are most likely represented by YS1 and YSL homologs. Future experiments should therefore focus on the membrane localization of YS1 and YSL proteins in graminaceous and dicotyledonous plants as well as on overexpression of *YS1* and *YSL* genes, which might become an important foundation for future phytoremediation strategies.

Acknowledgments—We thank Catherine Curie for providing the ZmYS1 cDNA clone, Günther Winkelmann for providing the *fet3 fet4* mutant, Dominique Loqué, Maria Ruckwied, and Nadine Drews for excellent technical assistance, and Toru Fujiwara, Junpei Takano, Wolfgang Schmidt, and Mike Merrick for critically reading the manuscript.

REFERENCES

1. Sugiura, Y., and Nomoto, K. (1984) *Struct. Bond.* **58,** 107–135
2. Neilands, J. B. (1995) *J. Biol. Chem.* **270,** 26723–26726
3. Braun, V., and Killmann, H. (1999) *Trends Biochem. Sci.* **24,** 104–109
4. Schmidt, W. (2003) *Trends Plant Sci.* **8,** 188–193
5. Toulon, V., Sentenac, H., Thibaud, J.-B., Soler, A., Clarkson, D., and Grignon, C. (1989) *Planta* **179,** 235–241
6. Römheld, V., and Marschner, H. (1986) *Plant Physiol.* **80,** 175–180
7. Ma, J. F., Kusano, G., Kimura, S., and Nomoto, K. (1993) *Phytochem.* **34,** 599–603
8. von Wirén, N., Mori, S., Marschner, H., and Römheld, V. (1994) *Plant Physiol.* **106,** 71–77
9. Curie, C., Panaviene, Z., Loulergue, C., Dellaporta, S. L., Briat, J.-F., and Walker, E. L. (2001) *Nature* **409,** 346–349
10. von Wirén, N., Marschner, H., and Römheld, V. (1995) *Physiol. Plant.* **93,** 611–616
11. Shi, W.-M., Chino, M., Youssef, R. A., Mori, S., and Takagi, S. (1988) *Soil Sci. Plant Nutr.* **34,** 585–592
12. Marschner, H. (1995) *Mineral Nutrition of Higher Plants*, Academic Press, London
13. Treeby, M., Marschner, H., and Römheld, V. (1989) *Plant Soil* **114,** 217–226
14. Römheld, V., and Awad, F. (2000) *J. Plant Nutr.* **23,** 1857–1866
15. Zhang, F., Römheld, V., and Marschner, H. (1991) *Soil Sci. Plant Nutr.* **37,** 671–678
16. von Wirén, N., Marschner, H., and Römheld, V. (1996) *Plant Physiol.* **111,** 1119–1125
17. Tolay, I., Erenoglu, B., Römheld, V., Braun, H. J., and Cakmak, I. (2001) *J. Exp. Bot.* **52,** 1093–1099
18. Shojima, S., Nishizawa, N. K., Fushiya, S., Nozoe, S., Irifune, T., and Mori, S. (1990) *Plant Physiol.* **93,** 1497–1503
19. Ling, H.-Q., Koch, G., Bäumlein, H., and Ganal, M. W. (1999) *Proc. Natl. Acad. Sci. U. S. A.* **96,** 7098–7103
20. von Wirén, N., Klair, S., Bansal, S., Briat, J.-F., Khodr, H., Shioiri, T., Leigh, R. A., and Hider, R. C. (1999) *Plant Physiol.* **119,** 1107–1114
21. Miyakoshi, K., Oshita, J., and Kitahara, T. (2001) *Tetrahedron* **57,** 3355
22. Sambrook, J., Fritsch, E. F., and Maniatis, T. (1989) *Molecular Cloning, A Laboratory Manual*, 2nd Ed., Cold Spring Harbor Laboratory Press, Cold Spring Harbor, NY
23. Rentsch, D., Laloi, M., Rouhara, I., Schmelzer, E., Delrot, S., and Frommer, W. B. (1995) *FEBS Lett.* **370,** 264–268
24. Ludewig, U., von Wirén, N., and Frommer, W. B. (2002) *J. Biol. Chem.* **277,** 13548–13555
25. Spizzo, T., Byersdorfer, C., Duesterhoeft, S., and Eide, D. (1997) *Mol. Gen. Genet.* **256,** 547–556
26. Rose, M. D., Winston, F., and Hieter, P. (1990) *Methods in Yeast Genetics*, Cold Spring Harbor Laboratory Press, Cold Spring Harbor, NY
27. Gietz, D., St. Jean, A., Woods, R. A., and Schiestl, H. (1992) *Nucleic Acids Res.* **20,** 1425
28. Eide, D., and Guarente, L. (1992) *J. Gen. Microbiol.* **138,** 347–354
29. Liu, L., Ludewig, U., Frommer, W. B., and von Wirén, N. (2003) *Plant Cell* **15,** 790–800
30. Eide, D., Broderius, M., Fett, J., and Guerinot, M. L. (1996) *Proc. Natl. Acad. Sci. U. S. A.* **93,** 5624–5628
31. Zhao, H., and Eide, D. J. (1997) *Mol. Cell Biol.* **17,** 5044–5052
32. Lubkowitz, M. A., Barnes, D., Breslav, M., Burchfield, A., Naider, F., and Becker, J. M. (2000) *Mol. Microbiol.* **28,** 729–741
33. Hauser, M., Donhardt, A. M., Barnes, D., Naider, F., and Becker, J. M. (2000) *J. Biol. Chem.* **275,** 3037–3041
34. Yen, M.-R., Teng, Y. H., and Saier, M. H., Jr. (2001) *Microbiology* **147,** 2881–2883
35. von Wirén, N., Khodr, H., and Hider, R. C. (2000) *Plant Physiol.* **124,** 1149–1157
36. Thibaud, J.-B., Davidian, J.-C., Sentenac, H., Soler, A., and Grignon, C. (1988) *Plant Physiol.* **88,** 1469–1473
37. Chrispeels, M. J., Crawford, M. N., and Schroeder, J. I. (1999) *Plant Cell* **11,** 661–676
38. Fischer, W.-N., Loo, D. D. F., Koch, W., Ludewig, U., Boorer, K. J., Tegeder, M., Rentsch, D., Wright, E. M., and Frommer, W. B. (2002) *Plant J.* **29,** 717–731
39. Vert, G., Grotz, N., Dédaldéchamp, F., Gaymard, F., Guerinot, M. L., Briat, J.-F., and Curie, C. (2002) *Plant Cell* **14,** 1223–1233
40. Conolly, E. L., Fett, J. P., and Guerinot, M. L. (2002) *Plant Cell* **14,** 1347–1357
41. Takahashi, M., Nakanishi, H., Kawasaki, S., Nishizawa, N. K., and Mori, S. (2001) *Nat. Biotechnol.* **19,** 466–469
42. Takahashi, M., Terada, Y., Nakai, I., Nakanishi, H., Yoshimura, E., Mori, S., and Nishizawa, N. K. (2003) *Plant Cell* **15,** 1263–1280
43. Walter, A., Pich, A., Scholz, G. Marschner, H., and Römheld, V. (1995) *J. Plant Nutr.* **18,** 1577–1593
44. Pich, A., Manteuffel, R., Hillmer, S., Scholz, G., and Schmidt, W. (2001) *Planta* **213,** 967–976
45. Thomine, S., Wang, R., Ward, J. R., Crawford, N M., and Schroeder, J. I. (2000) *Proc. Natl. Acad. Sci. U. S. A.* **97,** 4991–4996
46. Mizuno, D., Higuchi, K., Sakamoto, T., Nakanishi, H., Mori, S., and Nishizawa, N. K. (2003) *Plant Physiol.* **132,** 1989–1997
47. Vacchina, V., Mari, S., Czernic, P., Marques, L., Pianelli, K., Schaumlöffel, D., Lebrun, M., and Lobinski, R. (2003) *Anal. Chem.* **75,** 2740–2745

Downloaded from http://www.jbc.org/ by guest on June 8, 2020

ZmYS1 Functions as a Proton-coupled Symporter for Phytosiderophore- and Nicotianamine-chelated Metals

Gabriel Schaaf, Uwe Ludewig, Bülent E. Erenoglu, Satoshi Mori, Takeshi Kitahara and Nicolaus von Wirén

J. Biol. Chem. 2004, 279:9091-9096.
doi: 10.1074/jbc.M311799200 originally published online December 29, 2003

Access the most updated version of this article at doi: 10.1074/jbc.M311799200

Alerts:
- When this article is cited
- When a correction for this article is posted

Click here to choose from all of JBC's e-mail alerts

This article cites 44 references, 20 of which can be accessed free at
http://www.jbc.org/content/279/10/9091.full.html#ref-list-1

Downloaded from http://www.jbc.org/ by guest on June 8, 2020